Spectrum of cellular responses to pyriplatin, a monofunctional cationic antineoplastic platinum(II) compound, in human cancer cells

Katherine S. Lovejoy[a], Maria Serova[b], Ivan Bieche[c], Shahin Emami[d], Maurizio D'Incalci[e], Massimo Broggini[e], Eugenio Erba[e], Christian Gespach[d], Esteban Cvitkovic[b], Sandrine Faivre[b], Eric Raymond[b*], Stephen J. Lippard[a*].

[a]Department of Chemistry, Massachusetts Institute of Technology, Cambridge, Massachusetts, 02139 USA; [b]RayLab-U728 and Department of Medical Oncology, Beaujon University Hospital, Clichy, France; [c]Laboratory of Molecular Genetics, Beaujon University Hospital, Clichy, France; [d]INSERM U482, Saint-Antoine Hospital, Paris, France; [e]MarioNegri Research Institute, Milan, Italy.

Running title: Pyriplatin in human cancer cell lines

Keywords: cisplatin, pyriplatin, cytotoxicity, apoptosis, cell cycle, anticancer activity, DNA adducts

Abbreviations: *cis*-diammine(pyridine)chloroplatinum(II) (cDPCP), inductively coupled plasma mass spectrometry (ICP-MS), mismatch repair (MMR), poly (ADP-ribose) polymerase (PARP), TATA box-binding protein (TBP)

Financial Support: Work in the lab of S.J. Lippard is supported by a grant from the US National Cancer Institute (CA034992).

*Corresponding Authors:
Prof. Stephen J. Lippard
Department of Chemistry, Massachusetts Institute of Technology, Cambridge, Massachusetts, 02139 USA
Email: lippard@mit.edu
Phone: +1-617-253-1892
Fax: +1-617-258-8150

Prof. Eric Raymond
RayLab-U728, Beaujon University Hospital, Clichy, France
Email: eric.raymond@bjn.aphp.fr
Phone: +33-1-4087-5614
Fax: +33-1-4087-5487

The authors declare no potential conflicts of interest.

Word count (excluding references): 4998
Abstract word count: 249
Figure count: 6
Table count: 4
References: 42
Supplementary data: 4 figures and 1 table

Abstract

Pyriplatin, *cis*-diammine(pyridine)chloroplatinum(II), a platinum-based antitumor drug candidate, is a cationic compound with anticancer properties in mice and is a substrate for organic cation transporters that facilitate oxaliplatin uptake. Unlike cisplatin and oxaliplatin, which form DNA cross-links, pyriplatin binds DNA in a monofunctional manner. The antiproliferative effects of pyriplatin, alone and in combination with known anticancer drugs (paclitaxel, gemcitabine, SN38, cisplatin, 5-fluorouracil), were evaluated in a panel of epithelial cancer cell lines, with direct comparison to cisplatin and oxaliplatin. The effects of pyriplatin on gene expression and platinum-DNA adduct formation were also investigated. Pyriplatin exhibited cytotoxic effects against human cell lines after 24 h (IC_{50}: 171 – 443 μM), with maximum cytotoxicity in HOP-62 non-small cell lung cancer cells after 72 h (IC_{50}: 24 μM). Pyriplatin caused a G2/M cell cycle block similar to that induced by cisplatin and oxaliplatin. Induction of apoptotsis and DNA damage response was supported by Annexin-V analysis and detection of phosphorylated Chk2 and H2AX. Treatment with pyriplatin increased CDKN1/p21 and decreased ERCC1 mRNA expression. On a platinum-per-nucleotide basis, pyriplatin DNA adducts are less cytotoxic than those of cisplatin and oxaliplatin. The mRNA levels of genes implicated in drug transport and DNA damage repair, including GSTP1 and MSH2, correlate with pyriplatin cellular activity in the panel of cell lines. Synergy occurred for combinations of pyriplatin with paclitaxel. Because its spectrum of activity differs significantly from those of cisplatin or oxaliplatin, pyriplatin is a lead compound for

developing novel drug candidates with cytotoxicity profiles unlike those of drugs currently in use.

Introduction

Three platinum compounds currently in use worldwide - cisplatin, carboplatin, and oxaliplatin (Figure 1) - have been developed with crucial support from the United States NCI, including screening by the NCI's 60-cell line panel (NCI60 screen) (1). This process, together with the NCI COMPARE program, identified clear differences in activity profiles and mechanisms of action between platinum compounds, thus enabling the grouping of platinum compounds according to such characteristics (2). The cisplatin activity profile is similar to that of other diammineplatinum(II) compounds and to alkylating agents such as melphalan and camptothecin analogs. The oxaliplatin activity profile is similar to that of other platinum compounds containing the *R*,*R*-1,2-diaminocyclohexane ligand, including the platinum(IV) drug tetraplatin, and is also similar to those of acridines, organic compounds currently being developed as anticancer drugs (2).

Other classes of platinum compounds with activity different from cisplatin, oxaliplatin, or carboplatin have been defined on the basis of the NCI60 screen. The activity of the platinum-pyridines defines one group, into which some polyplatinum compounds including the clinically tested BBR3464 can be classified (3, 4). The platinum-silanes are another distinct group. Cells resistant to compounds from one group are commonly not cross-resistant to compounds from another. Similarly, because

of the different mechanisms of action for each type of compound, it is possible for compounds of different groups to be used in combination with synergistic results, an example being the synergistic effect of combining cisplatin and oxaliplatin (2). The development of platinum compounds with mechanisms of action different from those of platinum-based drugs already on the market should facilitate identification of candidate compounds that are active in cancers for which cisplatin, carboplatin, or oxaliplatin are inactive. Unique mechanisms of action may derive from the mode of cellular uptake of the compound (5), preferential localization of the platinum compound to a specific body organ or cell organelle (6), manipulation of the cellular response to enhance cytotoxicity (7), or the prevention or retardation of drug inactivation by biotransformation, as occurs for platinum(IV) prodrugs (8-10).

Pyriplatin is a monofunctional, cationic platinum(II) compound that has previously shown antitumor activity in mice (11), and which forms only a single covalent bond with DNA, unlike cisplatin, carboplatin, or oxaliplatin, which bind in a bidentate manner. Besides of this non-traditional structure, there is also evidence for a unique cellular mode of pyriplatin uptake that differs from the uptake of cisplatin or oxaliplatin. Pyriplatin is an outstanding substrate for the organic cation transporters (OCT) 1 and 2 (12, 13), which are associated with improved oxaliplatin uptake (14). Additionally, OCT1 has been identified as important to the pharmacokinetics and tissue distribution of pyriplatin (12). The mechanism of RNA polymerase II inhibition by pyriplatin-DNA adducts is dramatically different from the inhibition seen with cisplatin-DNA adducts (15), and the low nucleotide excision repair rates of the pyriplatin-DNA adduct, coupled

with its inhibition of RNA polymerase II (13), are very likely important to the cytotoxic mechanism of action. The aim of the present study was to further characterize pyriplatin *in vitro* with direct comparison to cisplatin and oxaliplatin to gain insight into the mechanism of action and potential clinical applications for pyriplatin. We investigated cellular and molecular changes induced by pyriplatin in order to determine possible response biomarkers and predictive factors of pyriplatin activity. The effects of combining pyriplatin with several anticancer drugs in current clinical use were also investigated.

Materials and Methods

Cell lines

All cell lines were obtained from the ATCC (Rockville, MD), and NCI cell collections. Cells were grown as monolayers in RPMI medium supplemented with 10% fetal calf serum (Invitrogen, Cergy-Pontoise, France), 2 mM glutamine, 100 units/ml penicillin and 100 µg/ml streptomycin. Cells were split twice a week using trypsin/EDTA (0.25%/0.02%; Invitrogen, Cergy-Pontoise, France) and seeded at a concentration of 2.5×10^4 cells/mL. All cell lines were tested regularly for *Mycoplasma* contamination by PCR using a Stratagene kit (La Jolla, CA).

Single agent evaluation

Pyriplatin was submitted to the National Cancer Institute (USA) for single agent, single dose testing in 2008. For evaluations performed in our laboratory, cells were seeded at 2×10^3 cells/well in 96-well plates and treated 24 h later with increasing concentrations

of cisplatin, oxaliplatin, or pyriplatin. After 1, 2, 5, 24, or 72 h of incubation, the cells were washed and post-incubated in platinum-free medium for 72 h (after 1, 2, or 5 h) or 48 h (after 24 or 72 h). Growth inhibition was then determined by the MTT assay (16). Absorption at 560 nm of the control wells containing untreated cells was defined as 100% and the viability of treated samples was expressed as a percentage of the control.

Cell cycle analysis

Exponentially growing MCF7 or HCT-116 cells were treated for 24 h with cisplatin, oxaliplatin, or pyriplatin at the IC_{50} concentrations (Table 1). At the end of treatment and following the 24, 48, or 72 h drug-washout period, the cells were counted, fixed in 70% cold ethanol, and kept at 4°C. The cells were washed with cold PBS and stained with 5 µg/mL propidium iodide in PBS and 12.5 µL/mL RNAse A. Flow cytometric cell cycle analysis was performed on a minimum of 2×10^4 cells per sample on a FACS Calibur instrument (Becton Dickinson, Sunnyvale, CA). A 488 nm laser and a dichroic mirror (570 nm) were used and fluorescence emission was detected using a filter for 620 ± 35 nm.

Evaluation of apoptosis

HCT-116 or MCF7 cells were harvested following 24 h treatment with platinum compounds at IC_{50} concentrations and 0, 24, 48, or 72 h of incubation in platinum-free medium. Cells were washed once with cold PBS, then pelleted and resuspended in 100 µL of a staining buffer containing Annexin V-FITC and 0.5 µg propidium iodide.

Fluorescence analysis by flow cytometry was performed after 15-minute incubation in the dark and dilution of the sample to 500 µL.

Western blotting

HOP-62 cells were treated for 24 h at the IC_{50} concentrations of pyriplatin, oxaliplatin, or cisplatin. The platinum-containing medium was removed and cells were lysed either immediately or 24, 48, or 72 h after removal of the platinum-containing medium. Following protein concentration quantification by the Bradford assay, extracts were analyzed on SDS-PAGE, transferred to PVDF membranes, incubated with primary antibodies, and revealed by peroxidase-coupled secondary antibodies using enzymatic chemiluminescence. Antibodies were obtained from commercial sources and used at the following dilutions: Ser^{139} phospho-H2AX (γ-H2AX, 1:1000, mouse monoclonal, Millipore-Upstate), Thr^{68} phospho-Chk2 (1:1000, rabbit polyclonal, Cell Signaling Technology), α-tubulin (1:10,000, mouse monoclonal, Amersham Biosciences), β-actin (1:20,000, mouse monoclonal, Sigma-Aldrich).

Combination evaluation

Antiproliferative effects of pyriplatin, cisplatin or oxaliplatin in combination with paclitaxel, gemcitabine, SN38, cisplatin, or 5-fluorouracil were investigated in the ovarian cancer line OVCAR-3 and the colon cancer line HT29. Combination studies were performed as described (17, 18). Briefly, cells were seeded at 2 x 10^3 cells/well in 96-well plates and incubated for 24 h prior to treatment. The combination experiments were performed on three different schedules. Cells were either treated with platinum for 24 h followed by the combination drug for 24 h, treated with the combination drug

for 24 h followed by platinum for 24 h, or treated for 24 h with pyriplatin and the combination drug simultaneously. Drug and platinum concentrations from IC_{20} to IC_{60} were used. Antiproliferative effects were evaluated by the MTT assay and analyzed using the Chou and Talalay method which is based on the median-effect principle (19) and the concentration-effect analysis CalcuSyn software (Biosoft, Cambridge, UK). A combination index (CI) of <1 indicates synergy, a value of 1 indicates additive effects, and a value >1 indicates antagonism.

Measurement of platinum content

HCT-116 cells were incubated for 2 or 24 h with 10 μM cisplatin, oxaliplatin, or pyriplatin. A time course of 2 h platinum exposure followed by a 22 h incubation in platinum-free medium (2/22 schedule) was also evaluated. After trypsinization, cytosol and nuclei were separated in a hypotonic buffer. Cell lysis was performed in a buffer of 100 mM Tris (pH 7.5) 1 mM EDTA, 1 mM EGTA, 0.5 mM Na_3VO_4, 10 mM sodium β-glycerophosphate, 50 mM sodium fluoride, 5 mM sodium pyrophosphate and 1% Triton X-100. DNA was purified from nuclear extracts by phenol-chloroform extraction and ethanol precipitation. Cellular lysates, DNA samples and incubation medium were analyzed for platinum levels by inductively-coupled plasma mass spectrometry (ICP-MS).

Quantitative RT-PCR analysis

HCT-116 cells were treated for 48 h with IC_{50} concentrations of drugs, followed by isolation of mRNA as described (20). Briefly, total RNA was reverse-transcribed before real-time quantitative PCR amplification using the ABI Prism 7900 Sequence Detection

System (Perkin-Elmer Applied Biosystems). The transcripts of the gene coding for the TATA box-binding protein (TBP; a component of the DNA-binding protein complex TFIID) were used as the endogenous control RNA for normalization. Results were expressed as N-fold differences in target gene expression relative to the TBP gene. The mRNA expression of ERCC1, XPA, XPC, PARP1, XRCC1, RAD50, BRCA1, DNA-PK-cs, XRCC6, MSH2, MLH1, BCL2, PUMA, COX2, CDKN1A/p21, ABCB1, ABCC1, GSTP1 was evaluated in a panel of 10 cancer cell lines. Thermal cycling was performed with an initial denaturation step at 95 °C for 10 min, and 50 cycles of 15 s at 95 °C and 1 min at 65 °C. Experiments were performed in duplicate.

Statistical analysis

Statistical analyses were performed with Instat and Prism software (GraphPad, San Diego, USA). Results are expressed as the mean ± standard deviation of at least three experiments performed in duplicate. Means and standard deviations were compared using the Student's *t*-test (two-sided *p* value).

Results

Antiproliferative effects of single agent pyriplatin in a panel of human cancer cell lines

The potential anticancer activity of pyriplatin was tested at the National Cancer Institute using the NCI-60 tumor cell line panel screen. Results are shown in Supplementary Figure S1. Analysis of these results using the online COMPARE algorithm revealed that the antiproliferative profile of pyriplatin was not similar to those of

cisplatin or oxaliplatin. The best correlation with a platinum compound in the NCI database was with "(carboxyphthalato) platinum" (NSC #S748451), with a correlation coefficient of 0.396. These data suggest that pyriplatin may have a mechanism of action that differs from classical platinum drugs.

Pyriplatin was further evaluated in comparison with cisplatin and oxaliplatin using a well-characterized panel (21) of 10 cancer cell lines of different tissue origins (colorectal, breast, melanoma, ovarian, non-small cell lung). Cells were exposed for 24 h to pyriplatin (0.46-1000 μM), cisplatin (0.1-160 μM), or oxaliplatin (0.1-160 μM) and assessed for cytotoxicity by the MTT assay. Cell counting and the sulforhodamine B assay (data not shown) confirmed the results of the MTT-based antiproliferative assays, shown in Table 1 as IC_{50} concentrations. The cytotoxicity profile for pyriplatin, shown in difference plots in Figure 2, was clearly different from those of both cisplatin and oxaliplatin.

To study the effects of duration of pyriplatin exposure on cell proliferation, we used the cell line in which pyriplatin showed the greatest antiproliferative effect (Figure 1). HOP-62 cells were treated for 1, 2, 5, 24, 48, or 72 h with pyriplatin, cisplatin or oxaliplatin, and then post-incubated for an additional 48 or 72 h period (as described above) in drug-free medium. Pyriplatin displayed dose- and time-dependent antiproliferative effects in HOP-62 cells, with a 72-h exposure producing the lowest IC_{50} value obtained for pyriplatin (IC_{50} = 24.3, Figure 3). The IC_{50} of pyriplatin was only 15-fold higher than that of cisplatin at 1 and 2 h, indicating that pyriplatin is clearly able to exert cytotoxicity after a short incubation period, unlike oxaliplatin. The difference

between pyriplatin and cisplatin increased at 5 h (IC_{50} of pyriplatin was 36-fold that of cisplatin) and at 24 h (53-fold difference), suggesting that pyriplatin loses efficacy over time relative to cisplatin.

Pyriplatin mechanism of action

To investigate the mechanism of pyriplatin cytotoxicity, cell cycle analyses were performed in HCT-116 and MCF7 cell lines. All three platinum compounds caused dose-dependent progressive accumulation of cells in the G2/M phases (see Figure 4A and Supplementary Figure S2). This block was apparent in both cell lines after a 24 h exposure to any of the three compounds, although oxaliplatin and pyriplatin induced only a slight G2/M block in MCF7 cells. The cells were able to repair this block at 72 h after washout, except at high concentrations of platinum. In the case of pyriplatin in HCT-116 cells, the effect was reversible after treatment with 35 or 70 μM pyriplatin, but not after treatment with 140 μM.

The implications of cell cycle disruption was explored by staining the cells with FITC-conjugated Annexin V for apoptosis detection and propidium iodide to detect necrosis prior to flow cytometric analysis. Annexin V binds to phosphatidylserine, a lipid that is present in the cell membrane of apoptotic cells. Cells were treated for 24 h with IC_{50} platinum concentrations (Table 1). Apoptosis was determined immediately following 24 h drug exposure (24hT) and at 24 h (24hR), 48 h (48hR), and 72 h (72hR) after drug washout. At 24hT drug exposure, the percentage of apoptotic cells in pyriplatin, cisplatin, and oxaliplatin-treated cells was approximately twice the control values (Table 2). The percentage of apoptotic cells peaked at 24 h after drug washout

for both cisplatin and pyriplatin-treated cells (24hR), and at 48h drug washout following oxaliplatin treatment (48hR). The detection of apoptosis 48 h after the start of exposure to cisplatin or 72 h after the beginning of incubation with oxaliplatin are in line with previously published results (22, 23). The peak of apoptosis in cells treated with pyriplatin corresponded to the maximal apoptotic response to cisplatin, suggesting that pyriplatin acts more quickly than oxaliplatin to induce cell death.

The effects of pyriplatin treatment on DNA damage response pathways related to cell cycle disruption and induction of apoptosis were explored by measuring levels of H2AX and Chk2 phosphorylation, p21 expression, and poly (ADP-ribose) polymerase (PARP-1) cleavage in HOP-62 cells by Western blotting after treatment with platinum at the IC_{50} concentrations. As a downstream substrate of ATM (24) and ATR (25), Chk2 is phosphorylated as part of the cellular response to cisplatin-induced DNA double-strand breaks (24). Phosphorylated H2AX (γ-H2AX) forms part of the repair complex that assembles at the site of DNA double-strand breaks and serves as a marker of DNA damage signaling (26). Cleavage of PARP-1 is observed in cells undergoing apoptosis (27) and produces two fragments of 89 and 24 kDa. Multiple roles of p21 and PARP-1 are also described in the context of DNA repair, regulation of cell cycle, apoptosis and gene transcription.

As shown in Figure 4B, increases in p21 and PARP levels as well as slight PARP cleavage were seen after exposure to pyriplatin for 24 h. γ-H2AX and Chk2 phosphorylation at Thr^{68} were detected following 24 h treatment with all three platinum compounds. Two bands were observed for γ-H2AX and persisted 72 h after removal of

the platinum-containing medium, corresponding to γ-H2AX at 15 kDa and ubiquitylated γ-H2AX at 25 kDa. The band at 25 kDa is shown in Figure 4B and both bands are presented in Figure S3. The high endogenous expression of phosphorylated H2AX in some tumor cell lines, including HOP-62, complicates the identification of induced DNA breaks using the band at 15 kDa (28, 29). The 25 kDa band is a ubiquitylated form of γ-H2AX, which is induced by the recently identified E3 ubiquitin ligase RNF168 (30). The 25 kDa band appears following cisplatin treatment of HCT-116 cells grown on fibronectin (31), and it is also induced upon cisplatin, oxaliplatin, or pyriplatin treatment of HOP-62 cells. Interestingly, ubiquitin-conjugated H2AX appear to accumulate at sites of DSBs, forming nuclear foci (30, 32). Ubiquitylation of histone H2AX is also critical for recruitment of important mediators of the DNA damage response, such as the MRN complex (*M*RE11, *R*AD50, and *N*BS1), the p53-binding protein 1 (53BP1) and BRCA1 (32, 33). Following DNA damage, the chromatin modifier ubiquitin ligase RNF168 colocalizes with γ-H2AX at DNA lesions and increases ubiquitylation of chromatin-associated proteins at the lesion site, promoting a downstream response to the DNA damage (30). The phosphorylation of γ-H2AX and Chk2 suggests the formation of DNA double strand breaks and indicates apoptotic DNA fragmentation or early DNA damage signaling events in response to treatment with pyriplatin. The pyriplatin-induced DNA damage-dependent ubiquitination of H2AX that is described indicates induction of a downstream DNA damage response to cell treatment with pyriplatin.

Molecular determinants of pyriplatin activity

Platinum levels on nuclear DNA were determined after exposure of HCT-116 cells to 10 μM pyriplatin for 2, 6, 24, and 48 h. Data were also obtained from cells exposed for 2h treatment followed by a 22-h incubation in platinum-free medium. Table 3 and Figure S4 show platinum content on DNA purified from these cells, as measured by ICP-MS. After a 2-h exposure, pyriplatin induced 3.1- and 1.3-fold fewer DNA adducts than cisplatin and oxaliplatin, respectively, indicating that pyriplatin is binding DNA quickly and supporting the results of cytotoxicity studies showing cytotoxicity of pyriplatin after only 1 or 2 h of treatment. Differences in adduct formation increased at 24 h and again at 48 h, with cisplatin forming 4- and 25-fold more adducts than pyriplatin at 24 and 48 h, respectively, and oxaliplatin forming 6- and 48-fold more adducts.

Comparing the 2-h incubation with the 2/22 schedule, DNA platination induced by pyriplatin and oxaliplatin is decreased by 68-70% after the 22-h washout period, whereas DNA platination in cisplatin-treated cells decreased to only 40%. Comparing the 2/22 schedule with the 24-h incubation, only slightly more pyriplatin-DNA adducts are observed at the 24 h mark, whereas larger increases in both cisplatin-DNA and oxaliplatin-DNA adducts are observed. Pyriplatin may be inactivated in the cell at a greater rate than either cisplatin or oxaliplatin, rendering less pyriplatin available for binding over time.

Overall, pyriplatin forms fewer DNA adducts than oxaliplatin and cisplatin, which may play a role in the reduced cytotoxicity of pyriplatin relative to the two established drugs. On the other hand, although pyriplatin is 66- to over 200-fold less potent than

cisplatin and oxaliplatin, respectively, at 24 h in HCT-116 cells, the difference in DNA adduct formation is not as stark, suggesting that each adduct of pyriplatin is less toxic than adducts of either cisplatin or oxaliplatin.

It was recently shown that exposure of colon cancer cells to oxaliplatin and cisplatin induced significant changes in expression of several genes implicated in drug transport, DNA repair, and cell cycle regulation (34). We compared the genetic effects induced by pyriplatin with those of oxaliplatin and cisplatin in the HCT-116 cell line**.** The mRNA levels encoded by selected genes involved in nucleotide excision repair (ERCC1, XPA, XPC), base excision repair (PARP1, XRCC1), homologous recombination (RAD50, BRCA1), mismatch repair (MSH2, MLH1), apoptosis (PUMA, CDKN1A/p21, COX2), transport (MDR1/ABCB1, ABCC1, GSTP1) and TOP2A, Ki67, and NEK2 were evaluated by RT-PCR after a 48-h exposure to pyriplatin, cisplatin, or oxaliplatin at IC_{50} concentrations. As shown in Figure 5 CDKN1/p21 mRNA expression was significantly induced following 48-h pyriplatin exposure (>3 fold). CDKN1/p21 mRNA levels were also induced after exposure to cisplatin and oxaliplatin, which is a well-characterized response to these drugs (35, 36). Additionally, induction of p21 is associated with cisplatin resistance in human testicular cancer (37). Pyriplatin also significantly decreased ERCC1 (2-fold decrease) expression. In contrast, exposure to cisplatin slightly increased the ERCC1 mRNA level (Figure 5), whereas exposure to oxaliplatin had little effect on ERCC1 mRNA. Pyriplatin-DNA adducts are repaired less efficiently by nucleotide excision repair than adducts of cisplatin with DNA (intrastrand d(GpG) crosslink) according to mammalian cell free extract-based assays (13). ERCC1 levels

may not be elevated in response to pyriplatin treatment because pyriplatin can largely evade repair by the ERCC1-associated nucleotide excision repair pathway The mRNA levels of other genes studied were not significantly affected (Figure 5 and data not shown).

The potential predictive role of various genes associated with pyriplatin sensitivity or resistance was investigated by plotting mRNA expression levels of 21 genes in the panel of 10 cell lines as measured by RT-PCR against pyriplatin IC_{50} values (Figure 6). In this case, cells were not treated with platinum prior to RT-PCR analysis. Although low levels of ERCC1 mRNA, but not necessarily the ERCC1 protein, are correlated with favorable responses of patients to a modified FOLFOX (biweekly oxaliplatin plus 5-FU and folinic acid) regimen (38), levels of ERCC1 mRNA were not correlated with response to pyriplatin. Cells with high levels of RAD50 mRNA are more resistant to pyriplatin (r^2 = 0.35), suggesting that double-strand breaks may play a role in the cellular consequences of pyriplatin-DNA lesions. Cells with high levels of mRNA coding for GSTP1 are also more resistant to pyriplatin (r^2 = 0.38), indicating possible cellular inactivation of pyriplatin by modification with glutathione. Genetic factors GSTP1 and RAD50 are slightly correlated with sensitivity to pyriplatin and may serve as predictive factors of response.

Pyriplatin in combination with other anticancer agents

The effect of administering pyriplatin prior to, subsequently to, and simultaneously with five commonly used anticancer agents in the HT29 and OVCAR-3 cell lines was evaluated after 24 h exposure and interpreted using the Chou and Talalay method. The colon adenocarcinoma HT29 and ovarian adenocarcinoma OVCAR-3 cell lines were

chosen because they represent two cancers for which platinum drugs are commonly effective; they have similar doubling times (20 h vs. 30 h) and relatively low sensitivity to pyriplatin (Table 1). Agents that had previously shown synergy in combination with platinum drugs were selected (17, 18) and combinatorial indices (CI) were calculated. A CI of less than 1, suggests that two drugs exert antiproliferative effects via separate mechanisms of action. Additive effects indicate that two drugs act via similar mechanisms of action.

A summary of pyriplatin-based combinations is shown in Table 4. Paclitaxel showed synergy (CI<1) when administered prior to pyriplatin in both cell lines. Similar to results for oxaliplatin and cisplatin (2), effects suggestive of synergy between pyriplatin and cisplatin were observed upon simultaneous addition of pyriplatin and cisplatin to cells (Table 4). Gemcitabine had antagonistic effects in both cell lines and with all schedules other than simultaneous exposure in HT29 cells.

Discussion

Platinum complexes are widely used in cancer therapy. The successful clinical applications of cisplatin, carboplatin, and oxaliplatin have inspired the synthesis and investigation of numerous platinum compounds as drug candidates. Of these compounds, those that show the most promise for clinical use have improved cytotoxicity, reduced side effects, or different mechanisms of action when compared with cisplatin, carboplatin, or oxaliplatin.

The cellular and molecular effects of the platinum derivative pyriplatin were investigated and directly compared to cisplatin and oxaliplatin. Because many variables such as passage number or culture conditions can affect the characteristics of a particular cell line, we ran parallel experiments with pyriplatin, cisplatin, and oxaliplatin on cells plated at the same time from a single flask. This experimental design produced data showing the unique anticancer profile of pyriplatin as compared and contrasted with those of cisplatin and oxaliplatin. The focus on comparisons between the platinum drugs freed us somewhat in the choice of cell line for various experiments, which were then made on the basis of wt p53 status (for apoptosis and cell cycle studies), sensitivity to pyriplatin (protein assays and cytotoxicity over time), and relevance to potential clinical use (combination assays).

The pyriplatin cytotoxicity profile is distinct from that of both cisplatin and oxaliplatin in a panel of 10 well-characterized cell lines and by the NCI single-dose screen. Although the IC_{50} values are 16 to 270 times higher for pyriplatin than for cisplatin or oxaliplatin, it is clear that the cell lines in which pyriplatin is most active (IGROV1, HOP-92, HOP-62, and COLO205) differ from those in which oxaliplatin is most active (HCT-116, OVCAR3, HOP-92, and MCF7) or those in which cisplatin is most active (HCT-116, HOP-92, HOP-62, and OVCAR3), as shown in the difference plots in Figure 2 and in Table 1. As is the case for cisplatin, the first cytotoxic effects of pyriplatin are seen as soon as one hour after the start of treatment, at which point pyriplatin is only 15-fold less toxic than cisplatin. Pyriplatin activity at 1 and 2 h contrasts with the relatively low activity of oxaliplatin, which must lose the oxalate prior to exerting

cytotoxic action and is significantly less active after 1 or 2 h than after 5 h or longer. Pyriplatin antiproliferative activity at 1 and 2 h is most likely related to the large number of platinum-DNA adducts observed by ICP-MS at the 2-h time point and the relatively swift induction of cell cycle arrest and apoptosis at only 48 h for pyriplatin, as opposed to 72 h for oxaliplatin. Measured IC_{50} values for pyriplatin decreased from 1 to 72 h, with efficacy peaking at an IC_{50} of 24 μM after 72 h in HOP-62 cells, the most sensitive cell line. Relative to cisplatin and based on IC_{50} values in HOP-62 cells, pyriplatin is about 15-fold less toxic than cisplatin after 1 or 2 h. This difference increases at 5 and 24 h, possibly pointing to deactivation of pyriplatin over time by cellular and molecular mechanisms. The affinity of thiols, including glutathione for platinum centers, is one probable method of deactivation of pyriplatin in the culture medium, and the single chloride on pyriplatin makes it more susceptible to complete deactivation by thiol coordination than cisplatin or oxaliplatin, which have two leaving groups and can still coordinate DNA if a thiol replaces one chloride ligand.

Cell cycle studies done in two cell lines with wt p53 status indicate that, similar to cisplatin and oxaliplatin, pyriplatin induces a G_2/M block that suggests cell cycle delay for a DNA damage response, DNA repair and/or apoptosis. Likewise, Annexin V staining and Western blots showing activation of proteins related to the cell cycle, DNA damage response and apoptosis indicate that pyriplatin also displays an apoptotic mechanism of action, as occurs for cisplatin and oxaliplatin. The detection of Annexin V bound to early-apoptotic cellular membranes 48 h after initiating cisplatin exposure or 72 h after oxaliplatin exposure are in line with previously published results (22, 23). The peak of

apoptosis in cells treated with pyriplatin corresponded to the maximal apoptotic response to cisplatin occurring 48 h after beginning treatment, suggesting that pyriplatin acts more quickly than oxaliplatin to induce cell death. The induction of H2AX phosphorylation confirms an early DNA damage signaling response to treatment with pyriplatin or may indicate the formation of dsDNA breaks in cells due to apoptotic DNA fragmentation.

When the effects of all three platinum compounds are compared at the same platinum concentration (10 μM), pyriplatin forms fewer DNA adducts than oxaliplatin or cisplatin after 24 h of treatment. However, after 2 h the levels of platinum per nucleotide are similar for pyriplatin and oxaliplatin. On the other hand, although pyriplatin is 66- to over 200-fold less potent than cisplatin and oxaliplatin respectively at 24 h in HCT-116 cells, the difference in DNA adduct formation is not as obvious, suggesting that each pyriplatin-DNA adduct is less toxic than adducts of cisplatin or oxaliplatin. Although the number of pyriplatin-DNA adducts is relatively similar to the number of cisplatin-DNA and oxaliplatin-DNA adducts, the antiproliferative effect of each adduct is significantly reduced. A promising route for development of cationic platinum anticancer compounds may involve replacing pyridine with bulkier heterocyclic amines. The X-ray structure of transcribing RNA polymerase II stalled at a site-specific pyriplatin-DNA adduct (15) is valuable for the purpose of predicting which new compounds will improve the transcription inhibition aspect of pyriplatin, an activity that is crucial to DNA damage signaling and eventual triggering of apoptosis. A research

program based on pyriplatin as a lead compound has already yielded compounds with significantly improved cytotoxicity compared to pyriplatin as well as cisplatin (39).

The cellular processing of platinum drugs involves a large number of cellular events that may play a role in the ultimate efficiency of these drugs: uptake and efflux, DNA adduct formation, recognition and repair of adducts, and signal transduction of DNA damage. In terms of molecular determinants of pyriplatin sensitivity, a slight correlation of pyriplatin IC_{50} with GSTP1 mRNA levels in untreated cells may indicate possible cellular inactivation of pyriplatin by glutathione modification. Levels of ERCC1 mRNA in untreated cells were not correlated with pyriplatin IC_{50}, which contrasts with the fact that low levels of ERCC1 mRNA are used to identify patients who are likely to respond well to a modified FOLFOX (biweekly oxaliplatin plus 5-FU and folinic acid) regimen (38).

Previously it was shown (25) that exposure of colon cancer cells to cisplatin and oxaliplatin can induce expression of several genes implicated in drug transport, DNA repair, and cell cycle regulation. We compared the genetic effects induced by pyriplatin with those induced by cisplatin and oxaliplatin in HCT-116 cells. Significant increases in p21 expression were seen for all three platinum compounds whereas ERCC1 expression decreased in response to pyriplatin and increased in response to cisplatin exposure. Because a high amount of ERCC1 is associated with resistance to cisplatin (40-42), the decrease in ERCC1 mRNA upon treatment with pyriplatin indicates a difference in cellular resistance to the two compounds. The difference in ERCC1 expression, coupled with previous results showing that pyriplatin-DNA adducts evade repair by the

nucleotide excision repair pathway as compared with repair of cisplatin-DNA adducts (13), supports the case that differential repair of cisplatin and pyriplatin adducts contribute to the different activity in our cell line panel.

The potential for use of pyriplatin in combination with other anti-cancer compounds was explored in terms of the antiproliferative potential of paclitaxel, gemcitabine, SN38, cisplatin, and 5-FU combinations. In both cell lines tested, pyriplatin was synergistic when administered simultaneously with cisplatin, as is seen when cells are treated with both cisplatin and oxaliplatin (2). Synergy implies a molecular mechanism of action distinct from that of cisplatin.

In conclusion, although pyriplatin is not likely to be developed due to its low cytotoxicity, it remains a promising lead compound for the generation of novel drug candidates with different cytotoxicity profiles from those of platinum drugs currently in use.

Acknowledgements

Data collected by ICP-MS was measured at the Salvatore Maugeri Foundation, Pavia, Italy. We acknowledge Dr Sarah MacKenzie for assistance in preparation of this manuscript.

References

1. Shoemaker RH. The NCI60 human tumour cell line anticancer drug screen. Nat Rev Cancer. 2006;6:813-23.
2. Rixe O, Ortuzar W, Alvarez M, Parker R, Reed E, Paull K, et al. Oxaliplatin, tetraplatin, cisplatin, and carboplatin: spectrum of activity in drug-resistant cell

lines and in the cell lines of the National Cancer Institute's Anticancer Drug Screen panel. Biochem Pharmacol. 1996;52:1855-65.

3. Roberts JD, Peroutka J, Farrell N. Cellular pharmacology of polynuclear platinum anti-cancer agents. J Inorg Biochem. 1999;77:51-7.
4. Farrell N, Qu Y, Bierbach U, Valsecchi M, Menta E. Structure-activity relationships within di- and trinuclear platinum phase-I clinical anticancer agents. In: Lippert B, editor. Cisplatin: Chemistry and Biochemistry of a Leading Anticancer Drug. Weinheim, Germany: Wiley-VCH; 1999. p. 479-96.
5. Hall MD, Okabe M, Shen D-W, Liang X-J, Gottesman MM. The role of cellular accumulation in determining sensitivity to platinum-based chemotherapy. Ann Rev Pharm Tox. 2008;48:495-535.
6. Molenaar C, Teuben J-M, Heetebrij RJ, Tanke HJ, Reedijk J. New insights in the cellular processing of platinum antitumor compounds, using fluorophore-labeled platinum complexes and digital fluorescence microscopy. J Biol Inorg Chem. 2000;5:655-65.
7. Barnes KR, Kutikov A, Lippard SJ. Synthesis, Characterization, and Cytotoxicity of a Series of Estrogen-Tethered Platinum(IV) Complexes. Chem Biol. 2004;11:557-64.
8. Hall MD, Mellor HR, Callaghan R, Hambley TW. Basis for Design and Development of Platinum(IV) Anticancer Complexes. J Med Chem. 2007;50:3403-11.
9. Reisner E, Arion VB, Keppler BK, Pombeiro AJL. Electron-transfer activated metal-based anticancer drugs. Inorg Chim Acta. 2008;361:1569-83.

10. Mukhopadhyay S, Barnes CM, Haskel A, Short SM, Barnes KR, Lippard SJ. Conjugated platinum(IV)-peptide complexes for targeting angiogenic tumor vasculature. Bioconjug Chem. 2008;19:39-49.
11. Hollis LS, Amundsen AR, Stern EW. Chemical and biological properties of a new series of cis-diammineplatinum(II) antitumor agents containing three nitrogen donors: cis-[Pt(NH3)2(N-donor) Cl]+. J Med Chem. 1989;32:128-36.
12. Li S, Chen Y, Zhang S, More SS, Huang X, Giacomini KM. Role of Organic Cation Transporter 1, OCT1 in the Pharmacokinetics and Toxicity of cis-Diammine(pyridine)chloroplatinum(II) and Oxaliplatin in Mice. Pharm Res. 2011;28:610-25.
13. Lovejoy KS, Todd RC, Zhang S, McCormick MS, D'Aquino JA, Reardon JT, et al. cis-diammine(pyridine)chloroplatinum(II), a monofunctional platinum(II) antitumor agent: uptake, structure, function, and prospects. Proc Natl Acad Sci U S A. 2008;105:8902-7.
14. Zhang S, Lovejoy KS, Shima JE, Lagpacan LL, Shu Y, Lapuk A, et al. Organic cation transporters are determinants of oxaliplatin cytotoxicity. Cancer Res. 2006;66:8847-57.
15. Wang D, Zhu G, Huang X, Lippard SJ. X-ray structure and mechanism of RNA polymerase II stalled at an antineoplastic monofunctional platinum-DNA adduct. Proc Natl Acad Sci USA. 2010;107:9584-9.

16. Hansen MB, Nielsen SE, Berg K. Re-examination and further development of a precise and rapid dye method for measuring cell growth/cell kill. J Immunol Methods. 1989;119:203-10.
17. Serova M, Calvo F, Lokiec F, Koeppel F, Poindessous V, Larsen AK, et al. Characterizations of irofulven cytotoxicity in combination with cisplatin and oxaliplatin in human colon, breast, and ovarian cancer cells. Cancer Chemother Pharmacol. 2006;57:491-9.
18. Raymond E, Buquet-Fagot C, Djelloul S, Mester J, Cvitkovic E, Allain P, et al. Antitumor activity of oxaliplatin in combination with 5-fluorouracil and the thymidylate synthase inhibitor AG337 in human colon, breast and ovarian cancers. Anti-Cancer Drugs. 1997;8:876-85.
19. Chou TC, Talalay P. Quantitative analysis of dose-effect relationships: the combined effects of multiple drugs or enzyme inhibitors. Adv Enzyme Regul. 1984;22:27-55.
20. Bieche I, Parfait B, Tozlu S, Lidereau R, Vidaud M. Quantitation of androgen receptor gene expression in sporadic breast tumors by real-time RT-PCR: evidence that MYC is an AR-regulated gene. Carcinogenesis. 2001;22:1521-6.
21. Serova M, Galmarini CM, Ghoul A, Benhadji K, Green SR, Chiao J, et al. Antiproliferative effects of sapacitabine (CYC682), a novel 2'-deoxycytidine-derivative, in human cancer cells. Br J Cancer. 2007;97:628-36.
22. Gatti L, Supino R, Perego P, Pavesi R, Caserini C, Carenini N, et al. Apoptosis and growth arrest induced by platinum compounds in U2-OS cells reflect a specific

DNA damage recognition associated with a different p53-mediated response. Cell Death Differ. 2002;9:1352-9.

23. Sharma RI, Smith TA. Colorectal tumor cells treated with 5-FU, oxaliplatin, irinotecan, and cetuximab exhibit changes in 18F-FDG incorporation corresponding to hexokinase activity and glucose transport. J Nucl Med. 2008;49:1386-94.

24. Pabla N, Huang S, Mi Q-S, Daniel R, Dong Z. ATR-Chk2 Signaling in p53 Activation and DNA Damage Response during Cisplatin-induced Apoptosis. J Biol Chem. 2008;283:6572-83.

25. Smith J, Tho LM, Xu N, Gillespie DA. The ATM-Chk2 and ATR-Chk1 pathways in DNA damage signaling and cancer. Adv Cancer Res. 2010;108:73-112.

26. Rogakou EP, Pilch DR, Orr AH, Ivanova VS, Bonner WM. DNA double-stranded breaks induce histone H2AX phosphorylation on serine 139. J Biol Chem. 1998;273:5858-68.

27. Kaufmann SH, Desnoyers S, Ottaviano Y, Davidson NE, Poirier GG. Specific proteolytic cleavage of poly(ADP-ribose) polymerase: an early marker of chemotherapy-induced apoptosis. Cancer Res. 1993;53:3976-63.

28. Banath JP, MacPhail SH, Olive PL. Radiation sensitivity, H2AX phosphorylation, and kinetics of repair of DNA strand breaks in irradiated cervical cancer cell lines. Cancer Res. 2004;64:7144-9.

29. Yu T, MacPhail SH, Banath JP, Klokov D, Olive PL. Endogenous expression of phosphorylated histone H2AX in tumors in relation to DNA double-strand breaks and genomic instability. DNA Repair. 2006;5:935-46.
30. Pinato S, Scandiuzzi C, Arnaudo N, Citterio E, Gaudino G, Penengo L. RNF168, a new RING finger, MIU-containing protein that modifies chromatin by ubiquitination of histones H2A and H2AX. BMC Mol Biol. 2009;10:55.
31. De Wever O, Sobczak-Thépot J, Vercoutter-Edouart A-S, Michalski J-C, Ouelaa-Benslama R, Stupack DG, et al. Priming and potentiation of DNA damage response by fibronectin in human colon cancer cells and tumor-derived myofibroblasts. Int J Oncol. 2011;Early Online.
32. Bergink S, Jentsch S. Principles of ubiquitin and SUMO modifications in DNA repair. Nature. 2009;458:461-7.
33. Hofmann K. Ubiquitin-binding domains and their role in the DNA damage response. DNA Repair. 2009;8:544-56.
34. Voland C, Bord A, Peleraux A, Penarier G, Carriere D, Galiegue S, et al. Repression of cell cycle-related proteins by oxaliplatin but not cisplatin in human colon cancer cells. Mol Cancer Ther. 2006;5:2149-57.
35. Vikhanskaya F, Colella G, Valenti M, Parodi S, D'Incalci M, Broggini M. Cooperation between p53 and hMLH1 in a human colocarcinoma cell line in response to DNA damage. Clin Cancer Res. 1999;5:937-41.

36. Zamble DB, Jacks T, Lippard SJ. p53-dependent and -independent responses to cisplatin in mouse testicular teratocarcinoma cells. Proc Natl Acad Sci U S A. 1998;95:6163-8.
37. Koster R, di Pietro A, Timmer-Bosscha H, Gibcus JH, van den Berg A, Suurmeijer AJ, et al. Cytoplasmic p21 expression levels determine cisplatin resistance in human testicular cancer. J Clin Invest. 2010;120:3594-605.
38. Wei J, Zou Z, Qian X, Ding Y, Xie L, Sanchez JJ, et al. ERCC1 mRNA levels and survival of advanced gastric cancer patients treated with a modified FOLFOX regimen. Br J Cancer. 2008;98:1398-402.
39. Park GY, Lippard SJ. Unpublished data. 2011.
40. Britten RA, Liu D, Tessier A, Hutchison MJ, Murray D. ERCC1 expression as a molecular marker of cisplatin resistance in human cervical tumor cells. Int J Cancer. 2000;89:453-7.
41. Dabholkar M, Vionnet J, Bostick-Bruton F, Yu JJ, Reed E. Messenger RNA levels of XPAC and ERCC1 in ovarian cancer tissue correlate with response to platinum-based chemotherapy. J Clin Invest. 1994;94:703-8.
42. Rosell R, Cobo M, Isla D, Sanchez Jose M, Taron M, Altavilla G, et al. Applications of genomics in NSCLC. Lung Cancer. 2005;50 Suppl 2:S33-40.

Tables

Table 1. Potency, expressed as IC_{50} concentrations, for pyriplatin, cisplatin, and oxaliplatin on cancer cell proliferation in a 10-cell line panel after 24-h incubation.

Cell Line	Cancer Type	IC_{50}		
		Pyriplatin	**Cisplatin**	**Oxaliplatin**
HOP-92	Non-Small Cell Lung	171 $\pm$ 56 μM	3.55 $\pm$ 3.2 μM	2.70 $\pm$ 0.60 μM
HOP-62	Non-Small Cell Lung	190 $\pm$ 36 μM	3.56 $\pm$ 1.4 μM	6.86 $\pm$ 0.39 μM
IGROV1	Ovarian	230 $\pm$ 33 μM	5.64 $\pm$ 1.3 μM	8.08 $\pm$ 2.9 μM
COLO 205	Colorectal	266 $\pm$ 57 μM	16.7 $\pm$ 7.2 μM	2.84 $\pm$ 0.64 μM
HCT-116	Colorectal	281 $\pm$ 50 μM	4.22 $\pm$ 2.5 μM	1.10 $\pm$ 0.28 μM
OVCAR-3	Ovarian	328 $\pm$ 128 μM	5.10 $\pm$ 3.0 μM	1.24 $\pm$ 0.30 μM
MCF7	Breast	335 $\pm$ 104 μM	15.6 $\pm$ 6.4 μM	1.70 $\pm$ 0.54 μM
HCC-2998	Colorectal	381 $\pm$ 103 μM	11.8 $\pm$ 4.0 μM	7.27 $\pm$ 2.3 μM
MDA-435	Breast /Melanoma	401 + 156 μM	5.81 + 4.0 μM	12.7 + 5.6 μM
HT29	Colorectal	443 + 255 μM	11.9 + 4.1 μM	6.65 + 1.0 μM

Data are means +/- SEM from three separate experiments, each performed in triplicate.

Table 2: Apoptosis induction according to Annexin V staining in MCF7 cells treated with pyriplatin, cisplatin, or oxaliplatin for 24 h followed by incubation in drug-free medium for 24, 48, or 72 h.

	Control	**Pyriplatin (25 µM)**	**Cisplatin (2 µM)**	**Oxaliplatin (0.4 µM)**
24hT	9.63%	16.84%	22.88%	18.02%
24hR	21.40%	51.70%	48.70%	21.94%
48hR	28.53%	32.57%	29.72%	35.42%
72hR	22.26%	16.66%	13.98%	16.76%

T=immediately after drug exposure, R=after wash-out. According to the experimental schedule, data are expressed as percentage of apoptotic cells. Corresponding data for HCT-116 cells are reported in the supporting information.

Table 3. DNA platinum content (ng Pt/mg DNA) of DNA extracted from HCT-116 cells after exposure to pyriplatin and analyzed by ICP-MS.

	2 h platinum	2 h platinum, 22 h washout	24 h platinum
pyriplatin	2.44	0.74	3.71
cisplatin	7.49	4.48	15.31
oxaliplatin	3.07	1.00	23.81

Table 4. Effects of pyriplatin in combination with various anticancer agents in HT29 and OVCAR-3 cancer cell lines.

Cell line	Schedule	Paclitaxel	Gemcitabine	SN38	Cisplatin	5-FU
HT29	**A**	**0.87 (0.75-0.98)**	1.66 (0.70-2.76)	0.90 (0.72-1.22)	1.11 (0.89-1.23)	0.94 (0.80-1.03)
	B	0.88 (0.69-1.22)	1.09 (0.89-1.38)	2.21 (1.42-3.31)	0.96 (0.94-1.22)	ND
	C	0.96 (0.55-1.21)	0.86 (0.45-1.49)	0.81 (0.62-1.34)	**0.84 (0.83-0.85)**	1.02 (0.87-1.20)
OVCAR-3	**A**	**0.89 (0.63-0.99)**	1.13 (0.69-1.91)	1.08 (1.51-0.77)	1.09 (0.96-1.19)	0.99 (0.89-1.22)
	B	1.06 (0.63-1.55)	1.31 (0.60-7.22)	0.95 (0.94-0.97)	0.84 (0.72-1.10)	ND
	C	1.19 (0.87-1.38)	1.21 (1.11-1.44)	1.38 (1.07-1.99)	**0.79 (0.74-0.85)**	1.32 (1.22-1.55)

ND=not determined

Data are presented as the median CI value and the 95% confidence interval. Schedule A: 24-h pyriplatin followed by the 24-h combination drug; Schedule B: 24-h combination drug followed by the 24-h pyriplatin; Schedule C: 24-h simultaneous exposure.

Figure legends

Figure 1. Structures of cisplatin, carboplatin, oxaliplatin, and pyriplatin.

Figure 2. Difference plot of antiproliferative effects of pyriplatin, cisplatin, and oxaliplatin in a panel of cancer cell lines. The indicated values are calculated as follows: log (IC_{50} individual cell line) – mean (log IC_{50}). Negative values indicate that the cell line is more sensitive than the average, whereas positive values indicate that the cell line is more resistant than the average.

Figure 3. Antiproliferative effects of pyriplatin, cisplatin, and oxaliplatin in HOP-62 cells over time. After 1, 2, 5, 24, or 72 h incubation, the cells were washed and post-incubated in platinum-free medium for 72 h (after 1, 2, or 5 h) or 48 (after 24 or 72 h). Cell viability was determined by the MTT assay. IC_{50} concentrations for different incubation times are shown as mean ± SD from at least three separate experiments.

Figure 4. Pyriplatin-induced cell cycle changes. A) Cell cycle analysis in HCT-116 cells treated with increasing pyriplatin concentrations; T=immediately after drug exposure, R=after washout. B) Western blot of DNA damage and apoptosis-related signaling protein expression in HOP-62 cells after a 24-h platinum treatment. β-actin was used as a loading control. Data are representative of 3 experiments.

Figure 5. Effects of pyriplatin, oxaliplatin, and cisplatin on gene expression. HCT116 cells were exposed to IC_{50} concentrations of pyriplatin, oxaliplatin and cisplatin for 48 hours. Relative mRNA gene expression of CDKN1/p21, XPA, TOP2A, NEK2, PUMA, ERCC1 was evaluated using quantitative RT-PCR. Data are representative of 3 experiments.

Figure 6. Correlation of pyriplatin cytotoxicity (IC_{50}s) and mRNA expression levels of GSTP1, RAD50, MLH1 and MSH2 in a panel of 10 cancer cell lines.

Figures

Figure 1.

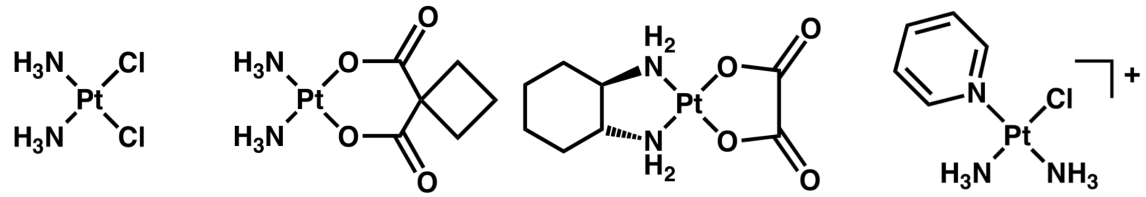

Cisplatin **Carboplatin** **Oxaliplatin** **Pyriplatin**

Figure 2.

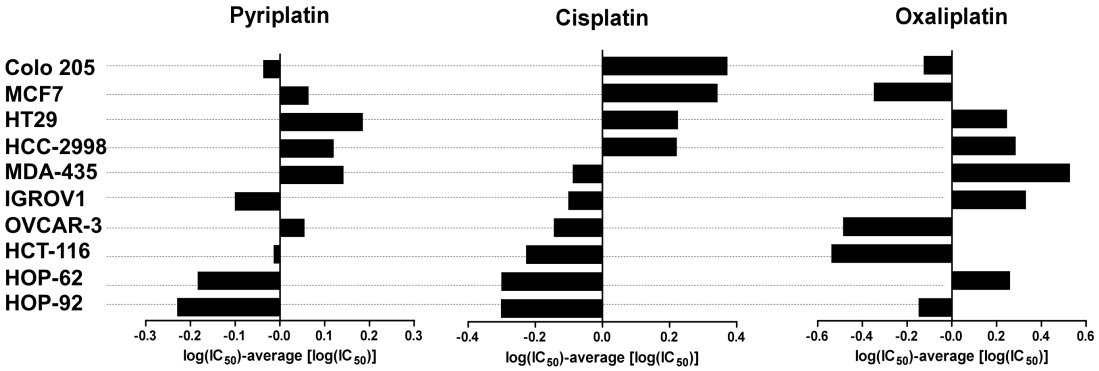
Pyriplatin
Cisplatin
Oxaliplatin
Colo 205
MCF7
HT29
HCC-2998
MDA-435
IGROV1
OVCAR-3
HCT-116
HOP-62
HOP-92
-0.3 -0.2 -0.1 -0.0 0.1 0.2 0.3
log(IC50)-average [log(IC50)]
-0.4 -0.2 0.0 0.2 0.4
log(IC50)-average [log(IC50)]
-0.6 -0.4 -0.2 -0.0 0.2 0.4 0.6
log(IC50)-average [log(IC50)]

Figure 3.

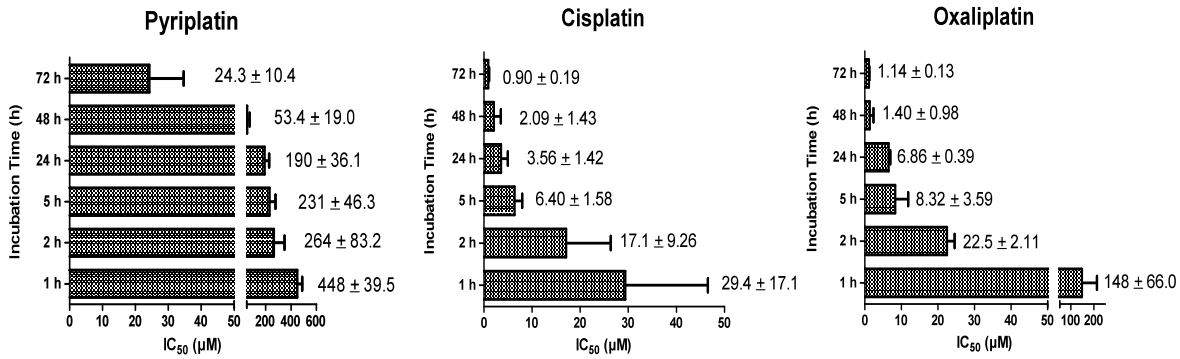
Pyriplatin
Cisplatin
Oxaliplatin
Incubation Time (h)
72 h
48 h
24 h
5 h
2 h
1 h
24.3 ± 10.4
53.4 ± 19.0
190 ± 36.1
231 ± 46.3
264 ± 83.2
448 ± 39.5
0.90 ± 0.19
2.09 ± 1.43
3.56 ± 1.42
6.40 ± 1.58
17.1 ± 9.26
29.4 ± 17.1
1.14 ± 0.13
1.40 ± 0.98
6.86 ± 0.39
8.32 ± 3.59
22.5 ± 2.11
148 ± 66.0
0 10 20 30 40 50 200 400 600
0 10 20 30 40 50
0 10 20 30 40 50 100 200
IC50 (μM)

Figure 4.

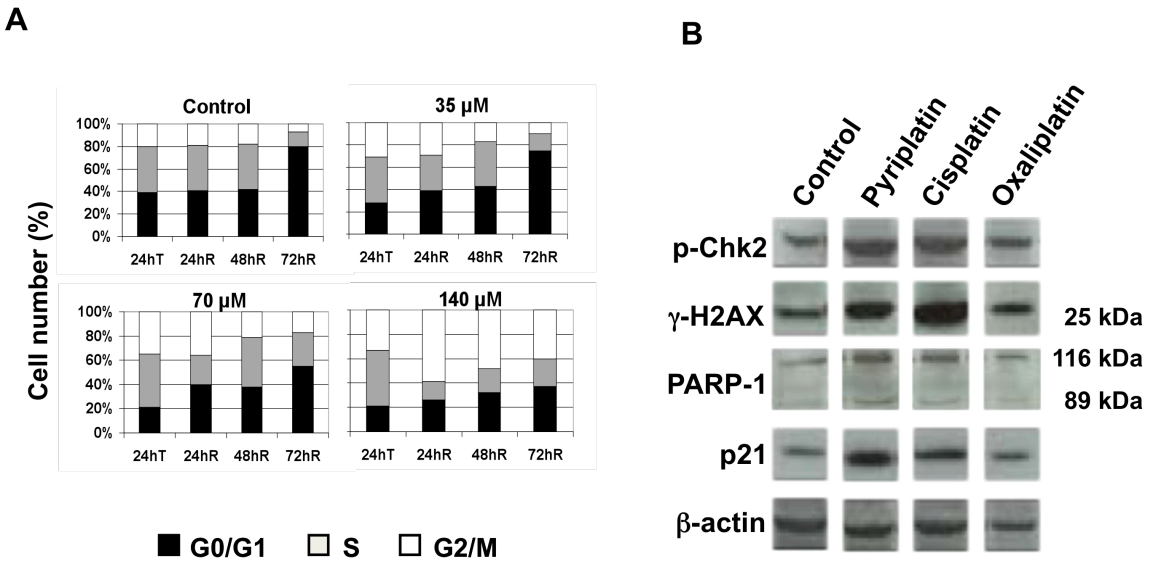
A
Control
35 μM
70 μM
140 μM
Cell number (%)
100%
80%
60%
40%
20%
0%
24hT
24hR
48hR
72hR
G0/G1
S
G2/M
B
Control
Pyriplatin
Cisplatin
Oxaliplatin
p-Chk2
γ-H2AX
PARP-1
p21
β-actin
25 kDa
116 kDa
89 kDa

Figure 5.

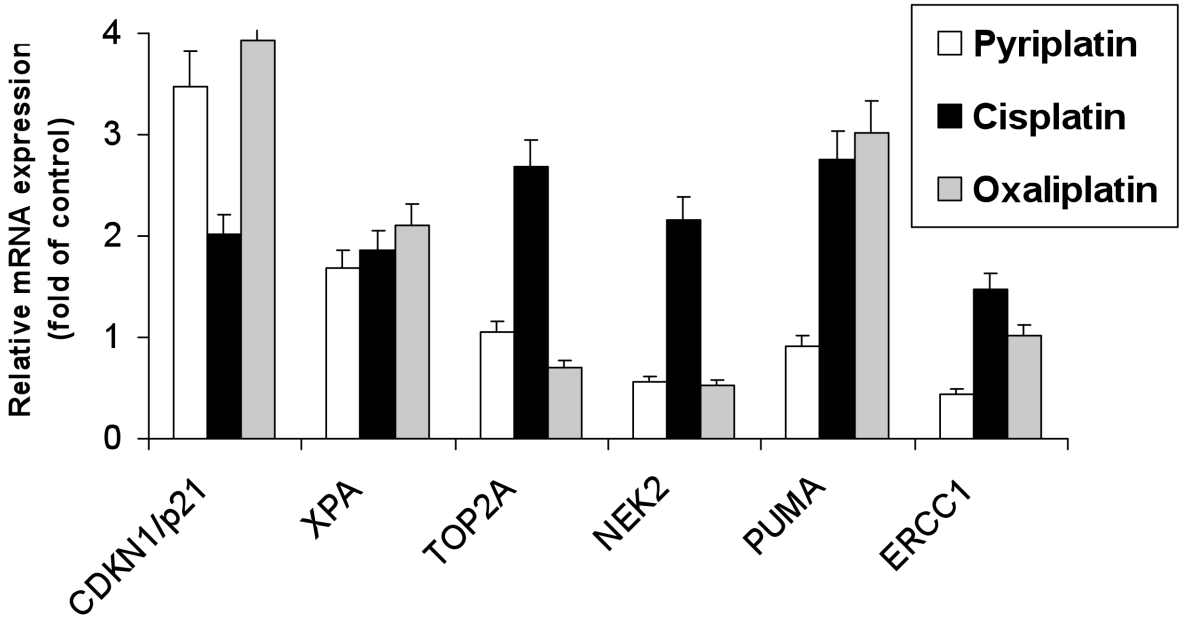
Relative mRNA expression
(fold of control)
0
1
2
3
4
CDKN1/p21
XPA
TOP2A
NEK2
PUMA
ERCC1
Pyriplatin
Cisplatin
Oxaliplatin

Figure 6.

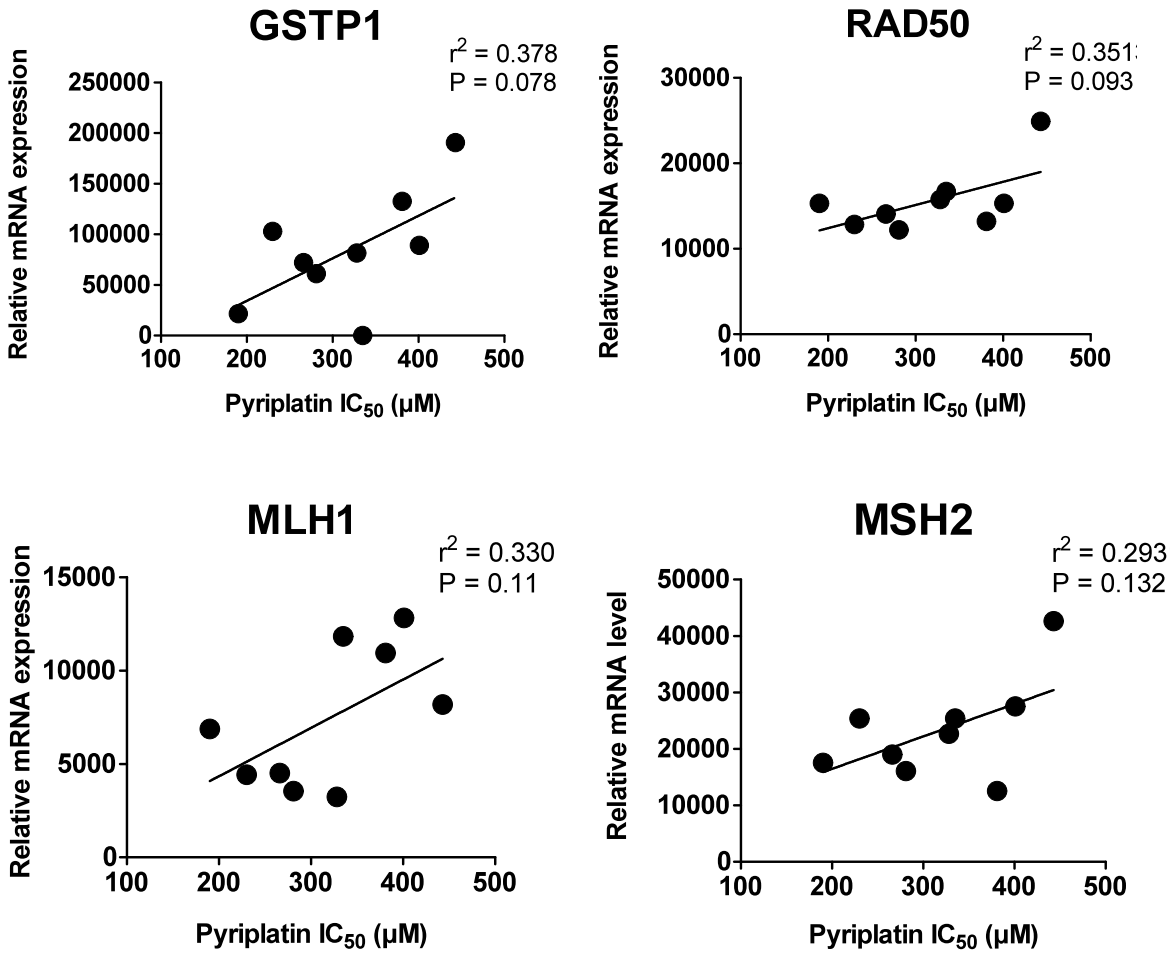
GSTP1
r2 = 0.378
P = 0.078
Relative mRNA expression
250000
200000
150000
100000
50000
0
100
200
300
400
500
Pyriplatin IC50 (μM)
RAD50
r2 = 0.351
P = 0.093
Relative mRNA expression
30000
20000
10000
0
100
200
300
400
500
Pyriplatin IC50 (μM)
MLH1
r2 = 0.330
P = 0.11
Relative mRNA expression
15000
10000
5000
0
100
200
300
400
500
Pyriplatin IC50 (μM)
MSH2
r2 = 0.293
P = 0.132
Relative mRNA level
50000
40000
30000
20000
10000
0
100
200
300
400
500
Pyriplatin IC50 (μM)